Journal of Pharmaceutical and Biomedical Analysis 53 (2010) 804–810

Contents lists available at ScienceDirect

Journal of Pharmaceutical and Biomedical Analysis

journal homepage: www.elsevier.com/locate/jpba

The interaction of sonochemically synthesized gold nanoparticles with serum albumins

Selvaraj Naveenraj [a], Sambandam Anandan [a,*], Arunkumar Kathiravan [b], Rajalingam Renganathan [b], Muthupandian Ashokkumar [c,**]

[a] Nanomaterials & Solar Energy Conversion Lab, Department of Chemistry, National Institute of Technology, Tiruchirappalli 620 015, India
[b] School of Chemistry, Bharathidasan University, Tiruchirappalli 620 024, India
[c] School of Chemistry, University of Melbourne, Grattan Street, Melbourne, Victoria 3010, Australia

ARTICLE INFO

Article history:
Received 29 December 2009
Received in revised form 24 March 2010
Accepted 25 March 2010
Available online 3 April 2010

Keywords:
Sonochemical reduction
Gold nanoparticles
Serum albumins
Fluorescence quenching

ABSTRACT

Spherical gold nanoparticles of approximately 16 nm were synthesized using a sonochemical reduction method and characterized using UV–vis spectroscopy, atomic force microscopy (AFM) and transmission electron microscopy (TEM). The binding of these gold nanoparticles with bovine serum albumin (BSA) and human serum albumin (HSA) was investigated using UV–vis absorption and fluorescence spectroscopic techniques. A strong quenching of the fluorescence from serum albumins was observed due to the formation of a ground state complex with gold nanoparticles (static quenching). The fluorescence quenching constants, number of binding sites and binding constants were determined using Stern–Volmer and Benesi–Hildebrand plots. Using Forster Resonance Energy Transfer (FRET) theory, the distance between the donor (serum albumins) and acceptor (gold nanoparticles) was obtained, which showed that HSA has more affinity towards sonochemically synthesized gold nanoparticles compared to gold nanoparticles synthesized using other methods.

1. Introduction

Nanotechnology, inextricably a multidisciplinary field, has an explosive growth in the past decade due to its extremely hefty applications in various fields of nanoscale electronics, optics, magnetics, energy, catalysis, nanomedicines, clothing, cosmetics, etc. [1]. Among all nanostructured materials, gold nanoparticles have attracted particular interest due to their stability, biocompatibility, surface plasmon resonance effect, and unique catalytic activities [2]. Owing to the unique optoelectronic properties with their controlled size and morphology, gold nanoparticles find significance in the field of bionanotechnology [6] as biomarkers [7], biosensors [8], cancer diagnostic [9] and vehicles for drug delivery [6]. Various preparation methods such as, seed growth, laser/photo irradiation, chemical vapour deposition, solvolysis, thermolytic reduction, solvothermal, sonochemical, electrochemical, chemical, microwave reduction, etc., have been employed in the synthesis of gold nanoparticles with the control of their size and morphology [3,4]. Among these synthetic methods, the sonochemical reduction drew particular attention due to the generation of nanoparticles with a smaller size range and higher surface area because of the unique reaction routes originating from transient high temperatures and pressures induced by the acoustic cavitation phenomenon [5].

Gold nanoparticles enhance the *in vitro* activities of antibacterial drugs such as vancomycin [10], ciproflaxin [11] and in addition shows antimicrobial activities due to its cytotoxicity towards various bacterial cells [12]. For the *in vivo* treatment of diseases, drugs have to be disseminated to the targeted tissues through the circulatory system. For this, serum albumins, the most abundant and major soluble protein constituent present in the blood stream of vertebrates, serve as a transport carrier of drugs due to their greater ability of binding reversibly with a large variety of endogenous and exogenous ligands present in blood [13]. Serum albumins (SA) including human serum albumin (HSA) and bovine serum albumin (BSA), posses numerous functionalities. Both BSA and HSA are 66 kDa globular proteins, consist of amino acid chains forming a single polypeptide with well-known sequence, which contain three homologous α-helices domains (I–III) assembled to form heart shaped molecules. HSA contains 585 amino acid residues with only one tryptophan (Trp) located at position 214 along the chain whereas BSA contains 582 amino acid residues with two tryptophans located in positions 134 and 212 in which Trp-212 is in chemical microenvironment similar to that Trp-214 in HSA and Trp-134 is located at the surface of the molecule [14–16].

* Corresponding author. Tel.: +91 431 2503639; fax: +91 431 2500133.
** Corresponding author. Tel.: +61 3 83447090; fax: +61 3 93475180.
E-mail addresses: sanand@nitt.edu, sanand99@yahoo.com (S. Anandan), masho@unimelb.edu.au (M. Ashokkumar).

0731-7085/$ – see front matter © 2010 Elsevier B.V. All rights reserved.
doi:10.1016/j.jpba.2010.03.039

Optical techniques play a vital role in the study of molecular interactions due to their sensitiveness and relative ease over the conventional approaches such as affinity and size exclusion chromatography, equilibrium dialysis, ultrafiltration and ultracentrifugation [15]. From the measurements and analyses of the fluorescence emission spectra, the fluorescence lifetime, fluorescence polarization, etc., detailed information can be gained about the structural fluctuations and the changes in the microenvironment surrounding macromolecules. For example, fluorescence spectroscopy plays a pivotal role in the investigation of interactions between a drug molecule and receptor proteins such as serum albumins since it allows non-intrusive substances in low concentration under the physiological conditions. For example, fluorescence quenching measurement reveals the accessibility of quenchers to albumin's fluorophore groups which in turn helps to understand albumin's binding mechanisms [16]. The reduction of the fluorescence intensity (quenching) of a given substance by the addition of a quencher may result from a variety of processes such as, excited state reactions, energy transfers, ground state complex formation and collisional deactivation processes [14]. It was theoretically predicted and experimentally observed that gold nanoparticles have ultrahigh fluorescence quenching ability [17].

In view of the fact that sonochemically synthesized nanoparticles have high surface area, enhanced binding interaction with serum albumins can be expected leading to a rapid transfer of drugs to the tissues. Hence, there is a fundamental interest in the study of *in vitro* binding interactions between serum albumins and sonochemically synthesized gold nanoparticles. For this reason, we studied the *in vitro* interactions of the sonochemically synthesised gold nanoparticles with serum albumins using UV–vis and fluorescence spectroscopic techniques.

2. Experimental

2.1. Materials

Chloroauric acid trihydrate ($HAuCl_4{\cdot}3H_2O$), HSA and BSA were purchased from Sigma–Aldrich. Serum albumin (BSA and HSA) solutions were prepared in pH 7.4 phosphate buffer solution and stored at 0–4 °C. All other reagents used were of analytical reagent grade. Water from a Milli Q apparatus (Millipore, USA) was used throughout the experiments. All the experiments were performed at atmospheric conditions.

2.2. Instrumentation

UV–vis absorption spectra were recorded with a T90+ UV–vis spectrophotometer (PG Instruments, United Kingdom). Fluorescence measurements were performed on a RF-5301 PC spectrofluorophotometer (SCHIMADZU, Japan). The samples were degassed using pure nitrogen gas for 15 min prior to each experiment. Fluorescence lifetime measurements were carried out in a picosecond time correlated single photon counting (TCSPC) spectrometer with a tunable Ti-sapphire laser (TSUNAMI, Spectra physics, USA) as the excitation source of 280 nm excitation wavelength. The fluorescence decay curves were analyzed using the software provided by IBH (DAS-6). The surface morphology and particle size of the sonochemically synthesized gold nanoparticles were analyzed using AFM (Nanoscope) and TEM (TECNAI G^2 model). About 2 drops of a solution containing the sonochemically synthesized gold nanoparticles were coated on a mica sheet at room temperature by drying with compressed N_2 gas for AFM studies. For TEM studies, samples were coated on copper grid at normal atmospheric conditions.

2.3. Procedures

2.3.1. Preparation of gold nanoparticles using sonochemical reduction

Gold nanoparticles were synthesized using a procedure reported by Yeung et al. [18]. An aqueous solution (70 mL) of $HAuCl_4{\cdot}3H_2O$ (0.2 mM) containing polyvinylpyrrolidone (0.1 wt%) and 2-propanol (0.1 M) was added to a sonication cell. Thermostated water was circulated through a water jacket attached to the cell thereby maintaining a constant temperature of about 20 °C. The solution was sonicated in continuous wave mode using a 20 kHz (23–47 W cm^{-3}) horn sonifier (Sonics) under nitrogen atmosphere for 30 min.

2.3.2. SA–gold nanoparticles interaction studies

Serum albumin concentration was kept constant at 4 μM and the concentration of sonochemically synthesized gold nanoparticles has been varied from 0 to 8 μM. This mixture was sonicated in an ultrasonic bath for 1 min. The interaction between SA and Au was monitored using UV–vis absorption and fluorescence spectroscopic techniques.

3. Results and discussion

3.1. Characterization of gold nanoparticles

The sonochemical reduction of Au(III) ions has been extensively studied and discussed in the literature by several groups [3,18–20]. The colour change of Au(III) solution during ultrasonic irradiation from pale yellow to the purple clearly indicated the formation of gold nanoparticles. It has already been reported that the sonochemical reduction of Au(III) is caused by the highly reactive free radicals generated during acoustic cavitation in aqueous solutions [18–20]. PVP solution was added to the reaction mixture for avoiding cluster formation during the synthesis of gold nanoparticles. UV–vis spectroscopy is the most extensively used method for characterizing the optical properties, electronic structure, particle size and surface structure of the nanoparticles. The UV–vis spectrum of the as-prepared purple coloured gold nanoparticles is shown in Fig. 1a. It exhibits a strong surface plasmon band at 532 nm, indicating the presence of spherical nanoparticles. The size of the sonochemically synthesized spherical gold nanoparticles was calculated from the UV–vis spectrum using Haiss equation [21] as follows:

$$d = \left(\frac{A_{spr}(5.89 \times 10^{-6})}{c_{Au}\ \exp(C_1)} \right)^{1/C_2}$$

where d is the diameter of the particle (nm), A_{spr} is the absorption at the surface plasmon band, c_{Au} is the amount of gold used in the synthesis (moles/L), $C_1 = -4.70$ and $C_2 = 0.314$. The size of the gold nanoparticle has been found out to be 15.6 nm using the absorption spectrum.

AFM is a high resolution imaging technique which is useful in the characterization of surface morphology of nanoparticles. Fig. 1b shows a typical AFM image of the sonochemically synthesized gold nanoparticles which are in the size range of 14–16 nm. It should be noted that gold nanoparticles are dispersed separately which reveals that nanoparticles did not aggregate due to the presence of PVP as a stabilizer. The TEM picture provided (Fig. 1c) indicates that the gold nanoparticles are essentially spherical and quasi-monodispersed with an average diameter of about 16 nm (the histogram of the TEM derived particle size distribution is shown as an inset in Fig. 1c). High resolution TEM image shown in Fig. 1d indicates the crystalline nature of the as-synthesized gold nanoparticles.

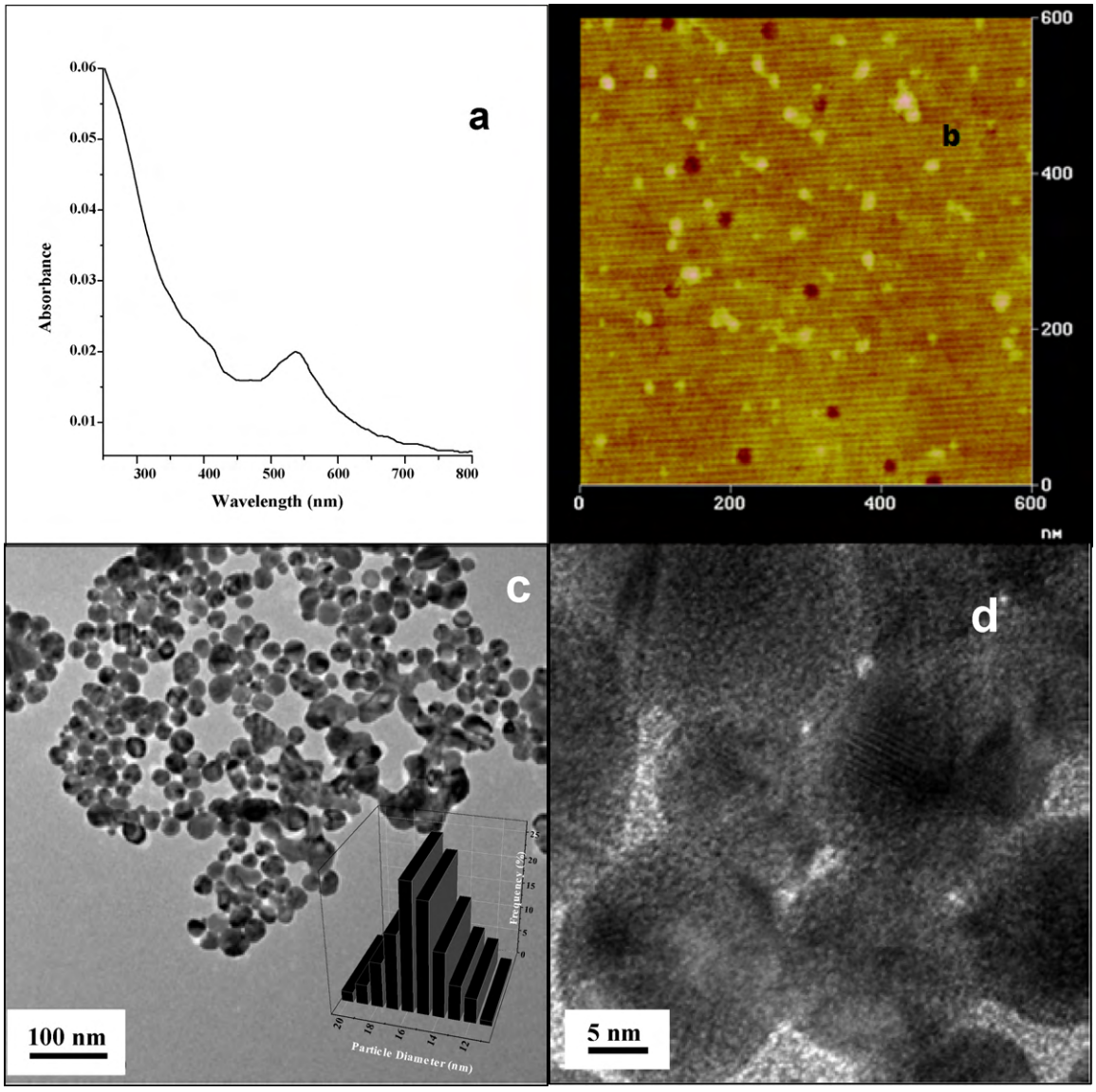

Fig. 1. Absorption spectrum (a), atomic force micrograph (b) and transmission electron micrographs (c and d) of sonochemically synthesized gold nanoparticles. TEM derived particle size distribution histogram is shown in the inset of Fig. 1c.

3.2. Absorption characteristics of serum albumin with gold nanoparticles

UV–vis absorption spectroscopy is a simple technique to explore the structural changes of molecules and to recognize the complex formation between different chemical entities [22]. Hence the absorption spectra of HSA and BSA in the presence of gold nanoparticles in the concentration range of 0–8 μM were recorded and shown in Fig. 2. It can be observed that due to the increase in the concentration of gold nanoparticles, the absorption around 532 nm increases accompanied with an increase in the absorption band at maximum around 280 nm with a slight blue shift in the peak location. Inset figure shows their absorption spectra normalized to 270–280 nm peak of a spectrum. Absorption of serum albumins at around 280 nm corresponds to absorption by tryptophan and tyrosine. The increase in the absorption at 280 nm is due the interaction between serum albumin and gold nanoparticles through a ground state complex formation, which is caused by the partial adsorption of SA on the surface of gold nanoparticles as reported in previous studies [22,23].

The equilibrium for the formation of the complex between serum albumins and gold nanoparticles can be given as shown below.

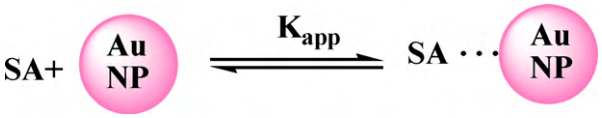

where K_{app} is the apparent association constant.

$$K_{app} = \frac{[SA\cdots Au]}{[SA][Au]} \quad (1)$$

The Benesi–Hildebrand equation [24] can be utilized to obtain K_{app} by using the changes in the absorption at 280 nm.

$$A_{obs} = (1-\alpha)C_0\varepsilon_{SA}l + \alpha C_0\varepsilon_{comp} \quad (2)$$

where A_{obs} is the observed absorbance of the solution containing different concentrations of gold nanoparticles at 280 nm. α is the degree of association between serum albumins and gold nanoparticles. ε_{SA} and ε_{comp} are the molar extinction coefficients of serum albumins and the SA–Au complex at 280 nm, respectively. By using

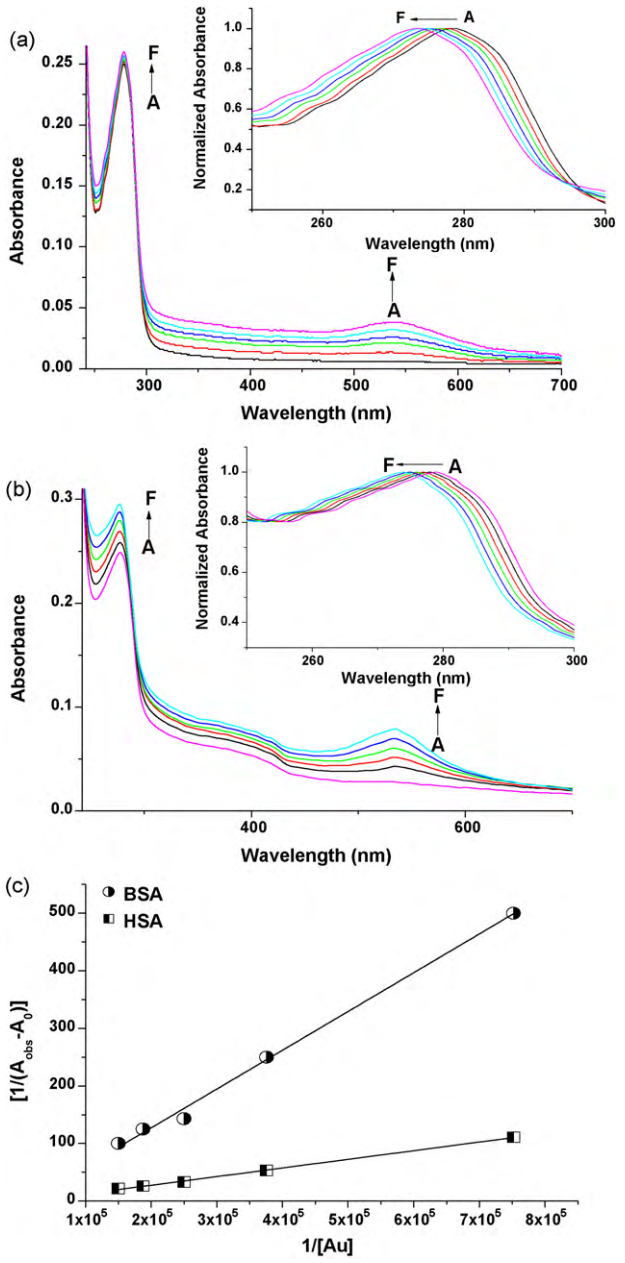

Fig. 2. Absorption spectra of serum albumin (4 μM) [(a) BSA and (b) HSA] in the absence and presence of gold nanoparticles in the concentration range of 0–8 μM. Inset shows their absorption spectra normalized to the 270–280 nm peak of a spectrum. Benesi–Hildebrand plots (c) for serum albumins in the presence of gold nanoparticles.

the Beer–Lambert law, we can write the above Eq. (2) as:

$$A_{obs} = (1 - \alpha)A_0 + \alpha A_{comp} \quad (3)$$

where A_0 and A_{comp} are the absorbances at 280 nm of serum albumin and the SA–Au complex, respectively. At relatively high gold nanoparticle concentrations, α can be defined as:

$$\alpha = \frac{K_{app}[Au]}{1 + K_{app}[Au]} \quad (4)$$

Hence at high concentrations of gold nanoparticles, the Eq. (3) can be modified to:

$$\frac{1}{A_{obs} - A_0} = \frac{1}{A_{comp} - A_0} + \frac{1}{K_{app}(A_{comp} - A_0)[Au]} \quad (5)$$

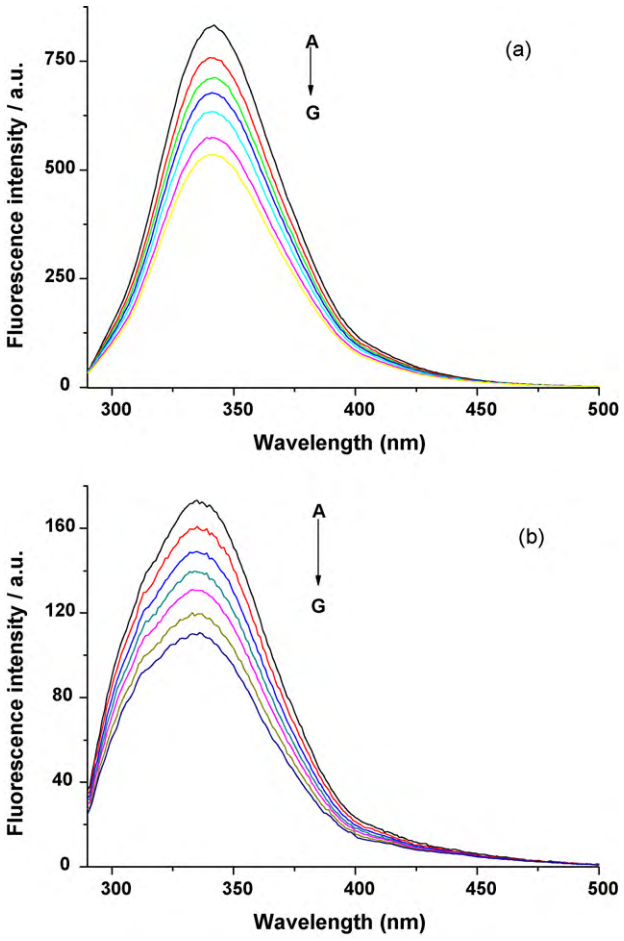

Fig. 3. The fluorescence spectra of serum albumin (4 μM) [(a) BSA and (b) HSA] solutions as a function of the concentrations of gold nanoparticles. The concentrations of gold nanoparticles utilized in A–G are 0, 1.33, 2.66, 4, 5.33, 6.66 and 8 μM, respectively.

Therefore, if the absorption enhancement at 280 nm is due to the absorption of complex, then a linear relationship should be obtained when $[1/(A_{obs} - A_0)]$ against 1/[Au] with a slope = $[1/K_{app}(A_{comp} - A_0)]$ and an intercept = $[1/(A_{comp} - A_0)]$. The values of apparent association constants determined (Fig. 2c) are $1.13 \times 10^4\ M^{-1}$ and $1.66 \times 10^4\ M^{-1}$ for BSA and HSA, respectively. The apparent association constant of HSA–Au is greater than that of BSA–Au, which signifies that HSA has more affinity than BSA towards gold nanoparticles.

3.3. *Fluorescence characteristics of serum albumins with gold nanoparticles*

The fluorescence emission of serum albumins originates from tryptophan (Trp), tyrosine (Tyr), and phenylalanine (Phe) moieties. However, the fluorescence of serum albumin is mainly contributed by the Trp moiety alone due to the low quantum yield of Phe and the total quenching of Tyr emission when it is self ionized or nearby an amino group, carboxylic acid, or Trp. The fluorescence characteristics are very sensitive to its microenvironment. It would be ultimately quenched if there is a slight change of the local surroundings of serum albumins, such as conformational transition, biomolecular binding, and denaturation. Hence, fluorescence spectra were recorded to assess the interaction of gold nanoparticles with serum albumins [25]. The effect of gold nanoparticles on the fluorescence spectra of serum albumins is shown in Fig. 3. It should be noted that the fluorescence intensity scales in Fig. 3a and b

are different. The fluorescence of serum albumin is mainly contributed by the tryptophan (Trp) moiety alone. As mentioned in Section 1, due to the presence of different number of Trp moiety, the fluorescence scales differ in Fig. 3a and b. It can be observed in Fig. 3 that with an increase in the concentration of gold nanoparticles from 0 to 8 μM, the fluorescence intensity of serum albumins gradually decreased without changing the emission maximum and shape of the band which indicates the binding of gold nanoparticles to serum albumins and the formation of non-fluorescent ground state complexes [22], as discussed earlier with regard to the UV–vis absorption spectra.

The normalized quenching intensities of serum albumins, i.e., F/F_0 ratio versus concentration of gold nanoparticles, are presented in Fig. 4a. At 1:1 molar ratio of gold nanoparticles/serum albumins, gold nanoparticles quench about 15% of HSA's fluorescence and about 19% of BSA's fluorescence. The extent of quenching reaches 25% when the concentration of gold nanoparticles was 1.6 times that of HSA and 1.3 times that of BSA. The fluorescence quenching can be better explained by the Stern–Volmer relation:

$$\frac{F_0}{F} = 1 + K_{SV}[Q] = 1 + k_q\tau_0[Q] \quad (6)$$

where F_0 and F are the fluorescence intensities of serum albumins in the absence and presence of Au; K_{SV}, k_q, and τ_0 are the Stern–Volmer quenching constant, bimolecular quenching rate constant and average lifetime of serum albumin (10^{-8} s), [Q] is the quencher concentration [22]. In Fig. 4b, the Stern–Volmer plots of serum albumins are shown. Within error limits, they both are linear. HSA titrated by gold nanoparticles shows linear Stern–Volmer plot with correlation coefficient $r = 0.9985$ ($P < 0.0001$) whereas BSA plot shows slightly concave curve upward ($r = 0.9841$, $P < 0.0001$). Linearity of HSA is due to either the existence of a binding site for gold nanoparticles in the proximity of tryptophan residue or the existence of more than one site spatially arranged so that they are equally accessible to gold nanoparticles whereas the non-linearity of BSA is due to the unequal accessibility of two tryptophan residues present in it to gold nanoparticles [14]. From the slopes of the linear plots, the Stern–Volmer quenching constants (K_{SV}) were calculated as 6.58×10^4 L mol^{-1} for BSA and 4.57×10^4 L mol^{-1} for HSA. The bimolecular quenching rate constants, k_q of BSA and HSA are found to be 6.58×10^{12} and 4.57×10^{12} L mol^{-1} s^{-1}, respectively. These k_q values are greater than that of scatter procedure (2×10^{10} L mol^{-1} s^{-1}) which shows that the quenching mentioned above is not initiated by dynamic collision but from the ground state complex formation of static quenching [22].

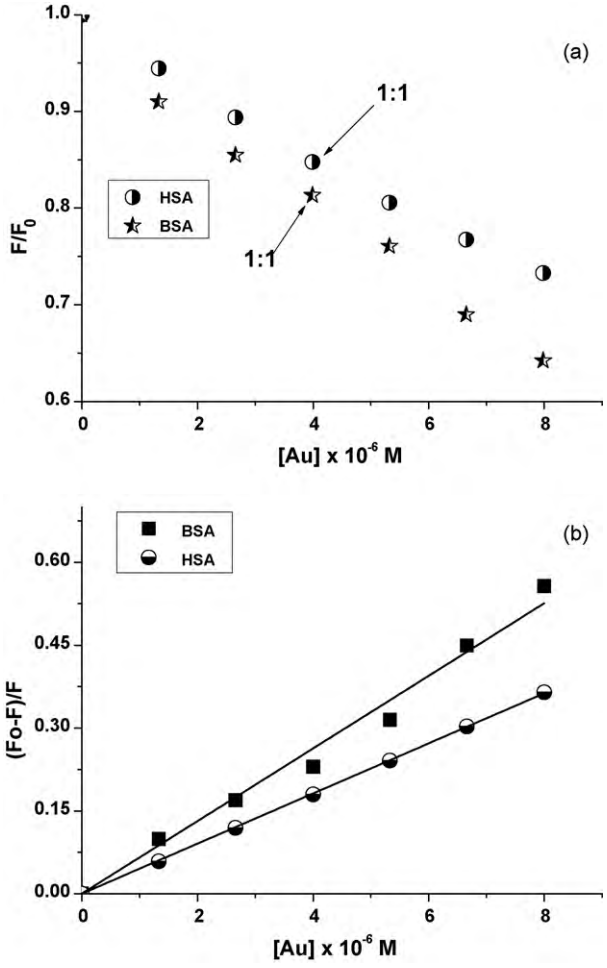

Fig. 4. Normalized quenching plot (a) and Stern–Volmer plot (b) for serum albumins in the presence of gold nanoparticles. The concentrations of gold nanoparticles utilized in A–G are 0, 1.33, 2.66, 4, 5.33, 6.66 and 8 μM, respectively.

The fluorescence quenching can either be dynamic or static, resulting from the collisional encounters or the ground state complex formation between the fluorophore and quencher, respectively. Static quenching can easily be distinguished from that of dynamic by their different binding constants dependence on temperature and viscosity, or preferably by lifetime measurements.

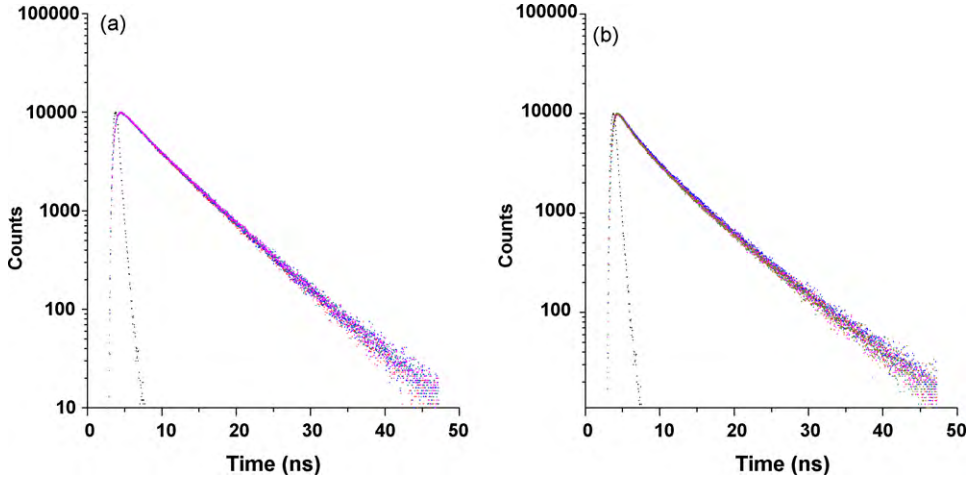

Fig. 5. Fluorescence decay curves of serum albumin (4 μM) [(a) BSA and (b) HSA] in the presence of gold nanoparticles in the concentration range of 0–8 μM.

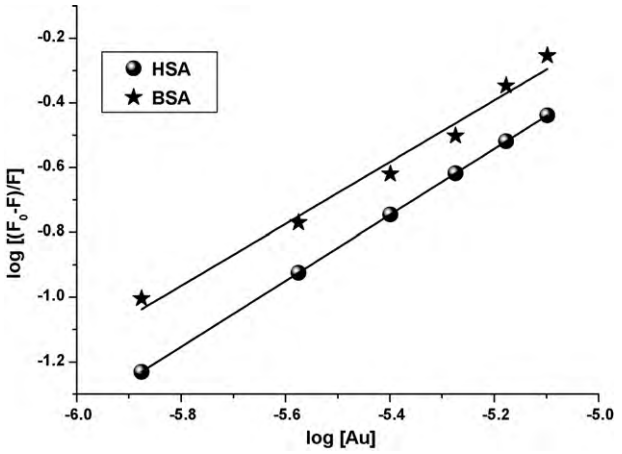

Fig. 6. log[$(F_0 - F)/F$] versus log[Q] plots for serum albumins versus gold nanoparticles.

In this study, we also used the lifetime measurements to further support the quenching mechanism as static. Fig. 5 shows the fluorescence decay of serum albumins (Fig. 5a: BSA; Fig. 5b: HSA) in the absence and presence of gold nanoparticles. Serum albumins exhibit double exponential decay even in the presence of gold nanoparticles. An increase in the concentration of gold nanoparticles had no effect in the lifetime of serum albumins. This behaviour reveals that the quenching follows static mechanism which supports the formation of ground state complex between serum albumins and gold nanoparticles.

3.4. Binding constants and the number of binding sites

The binding constant (K) and the number of binding sites (n) between gold nanoparticles and serum albumins can be calculated using the equation for the static quenching process:

$$\log\left[\frac{F_0 - F}{F}\right] = \log\ K + n\ \log[Q] \tag{7}$$

A plot of log[$(F_0 - F)/F$] versus log[Q], shown in Fig. 6, gives a straight line where the slope and the intercept corresponding to n and log K, respectively. The values of K and n have been found out to be 3.71×10^4 L mol^{-1} and 0.9545 for BSA and 5.68×10^4 L mol^{-1} and 1.019 for HSA. HSA binding constant with sonochemically synthesized gold nanoparticles is found to be about 1.5 times greater than that of BSA. This indicates that affinity of HSA is more than that of BSA towards gold nanoparticles synthesized by sonochemical reduction where in the case of gold nanoparticles synthesized by $NaBH_4$ reduction method, BSA showed more affinity than that of HSA [25]. According to literature [14,25], and supported by the non-linear BSA Stern–Volmer plot, this decrease effect of binding constant is due to the primary binding site of gold nanoparticles for BSA located asymmetrically between the two tryptophan residues compared to HSA containing one tryptophan moiety. From the number of binding sites (n is almost constant =1), we can conclude that there was one independent class of binding sites on serum albumins for gold nanoparticles and it formed a 1:1 complex with the serum albumin molecule.

The fluorescence quenching of serum albumins after binding with gold nanoparticles indicated the occurrence of energy transfer between gold nanoparticles and serum albumins, a significant criterion used to evaluate the distance between the ligand and the tryptophan moiety in the protein by means of the Forster resonance energy transfer theory (FRET). According to FRET, transfer of energy, which occurs through direct electrodynamic interaction between the primarily excited molecules and their neighbours, is controlled by the following three aspects: (1) the donor should have strong fluorescence quantum yield, (2) more spectral overlap between the donor emission and the acceptor absorption, (3) the distance (r) between the acceptor and the donor should be within 7 nm. This theory points out that the energy transfer efficiency 'E', in addition to its dependence on the distance between the acceptor and the donor, it also depends upon the critical energy transfer distance, R_0 (Förster's distance; the distance at which the efficiency of energy transfer is 50%), which is expressed by the following equation:

$$E = 1 - \frac{F}{F_0} = \frac{R_0^6}{R_0^6 + r_0^6} \tag{8}$$

The magnitude of R_0 is dependent on the spectral characteristics of the donor emission and acceptor absorption of the molecules. R_0 is expressed as follows:

$$R_0^6 = 8.8 \times 10^{-25}[\kappa^2 N^{-4} \phi_D J] \tag{9}$$

where κ^2 is the spatial orientation factor related to the geometry of the donor and acceptor of dipoles, $\kappa^2 = 2/3$ for random orientation as in fluid solution, N is the refractive index of the medium (1.36 for BSA and 1.336 for HSA), ϕ_D is the fluorescence quantum yield of the donor (0.118 for BSA and 0.15 for HSA), J is the overlap integral of the fluorescence emission spectrum of the donor serum albumins and the absorption spectrum of the acceptor gold nanoparticles

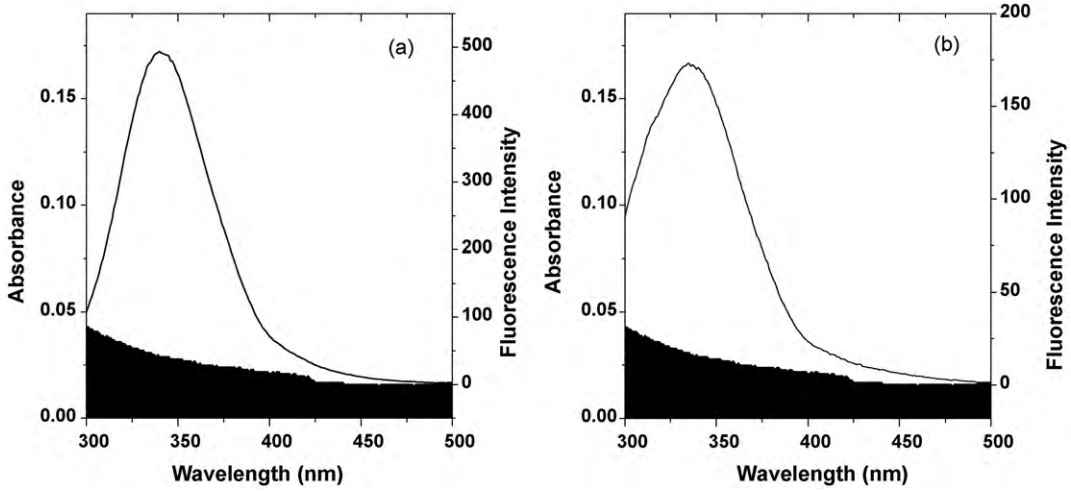

Fig. 7. Overlap plots of fluorescence spectra of serum albumins (a) BSA and (b) HSA with absorption spectra of gold nanoparticles.

(Fig. 7), which could be calculated by the equation:

$$J = \frac{\int_0^\infty F(\lambda)\varepsilon(\lambda)\lambda^4 \, d\lambda}{\int_0^\infty F(\lambda)\, d\lambda} \quad (10)$$

where $F(\lambda)$ is the corrected fluorescence intensity of the donor in the wavelength range from λ to $(\lambda + \Delta\lambda)$, with the total intensity normalized to unity and $\varepsilon(\lambda)$ is the molar extinction coefficient of the acceptor at λ. Using Eqs. (8)–(10), that the following values were obtained: $R_0 = 3.92$ nm, $E = 0.22$ and $r_0 = 4.83$ nm for BSA and $R_0 = 4.6$ nm, $E = 0.19$ and $r_0 = 5.75$ nm for HSA. The donor-to-acceptor distance, $r_0 < 7$ nm and $0.5R_0 < r_0 < 1.5R_0$, indicated that the energy transfer from serum albumins to gold nanoparticles occurs with high probability [22]. This again supports the static quenching mechanism.

4. Conclusion

Using a simple sonochemical reduction method, we have synthesized gold nanoparticles of size ~16 nm which were characterized by UV–vis spectroscopy, AFM and TEM. The interaction of globular fluorescent protein serum albumins, BSA and HSA, with sonochemically synthesized gold nanoparticles has been extensively studied using absorption and fluorescence spectroscopic techniques. Experimental results confirmed that the quenching of the fluorescence emission from serum albumins by gold nanoparticles follows a static quenching mechanism and gold nanoparticles bind to serum albumins with high affinity. The binding constants obtained from modified Stern–Volmer plots and the apparent association constants from Benesi–Hildebrand plots suggested that HSA has more affinity towards sonochemically synthesized gold nanoparticles than that of BSA. The distance between the serum albumins and gold nanoparticles has also been calculated using FRET. This binding study is biologically significant since serum albumins are used as drug carriers and gold nanoparticles possess antimicrobial activities. Hence, this report has a great significance in pharmacology and clinical medicine.

Acknowledgements

Authors SA and MA thank DST, New Delhi (INT/AUS/P-1/07 dated 19th Sep 2007) and DEST, Australia for the sanction of INDIA-AUSTRALIAN strategic research fund for their collaborative research. Also the authors thank Prof. P. Ramamurthy, Director, National Centre for Ultra Fast Processes, University of Madras, Taramani Campus, Chennai, India for analysing lifetime measurements.

References

[1] P.G. Luo, F.J. Stutzenberger, Nanotechnology in the detection and control of microorganisms, Adv. Appl. Microbiol. 63 (2008) 145–181.
[2] X. Lu, H. Tuan, B.A. Korgel, Y. Xia, Facile synthesis of gold nanoparticles with narrow size distribution by using AuCl or AuBr as the precursor, Chem. Eur. J. 14 (2008) 1584–1591.
[3] S. Anandan, F. Grieser, M. Ashokkumar, Sonochemical synthesis of Au–Ag core–shell bimetallic nanoparticles, J. Phys. Chem. C 112 (2008) 15102–15105.
[4] C. Feng, L. Gu, D. Yang, J. Hu, G. Lu, X. Huang, Size-controllable gold nanoparticles stabilized by PDEAEMA-based double hydrophilic graft copolymer, Polymer 50 (2009) 3990–3996.
[5] K.S. Suslick (Ed.), Ultrasound: Its Chemical, Physical, and Biological Effects, VCH, Weinheim, Germany, 1988.
[6] R.A. Sperling, P.R. Gil, F. Zhang, M. Zanella, W.J. Parak, Biological applications of gold nanoparticles, Chem. Soc. Rev. 37 (2008) 1896–1908.
[7] H. Wan, L. Chen, J. Chen, H. Zhou, D. Zhang, L. Liu, Synthesis and fluorescence property of the gold nanoparticles modified with 9-methyl-9-(8-thiooctyl)-fluorene, J. Dispersion Sci. Technol. 29 (2008) 999–1002.
[8] S. Tokonami, H. Shiigi, T. Nagaoka, Preparation of nanogapped gold nanoparticle array for DNA detection, Electroanalysis 20 (2008) 355–360.
[9] X. Huang, P.K. Jain, I.H. El-Sayed, M.A. El-Sayed, Gold nanoparticles: interesting optical properties and recent applications in cancer diagnostics and therapy, Nanomedicine 2 (2007) 681–693.
[10] H. Gu, P.L. Ho, E. Tong, L. Wang, B. Xu, Presenting vancomycin on nanoparticles to enhance antimicrobial activities, Nano Lett. 3 (2003) 1261–1263.
[11] R.T. Tom, V. Suryanarayanan, P.G. Reddy, S. Baskaran, T. Pradeep, Ciprofloxacin-protected gold nanoparticles, Langmuir 20 (2004) 1909–1914.
[12] Y. Zhang, H. Peng, W. Huang, Y. Zhou, D. Yan, Facile preparation and characterization of highly antimicrobial colloid Ag or Au nanoparticles, J. Colloid Interface Sci. 325 (2008) 371–376.
[13] H. Gao, L. Lei, J. Liu, Q. Kong, X. Chen, Z. Hu, The study on the interaction between human serum albumin and a new reagent with antitumour activity by spectrophotometric methods, J. Photochem. Photobiol. A: Chem. 167 (2004) 213–221.
[14] D. Silva, C.M. Cortez, S.R.W. Louro, Chloropromazine interactions to sera albumins A study by the quenching of fluorescence, Spectrochim. Acta A: Mol. Biomol. Spectrosc. 60 (2004) 1215–1223.
[15] Y. Li, W. He, J. Liu, F. Sheng, Z. Hu, X. Chen, Binding of the bioactive component Jatrorrhizine to human serum albumin, Biochim. Biophys. Acta 1722 (2005) 15–21.
[16] C. Wang, Q. Hu, C. Li, Z. Wang, J. Ma, X. Zang, Interaction of tetrandine with human serum albumin: a fluorescence quenching study, Anal. Sci. 23 (2007) 429–433.
[17] S. Song, Z. Liang, J. Zhang, L. Wang, G. Li, C. Fan, Gold-nanoparticle-based multicolor nanobeacons for sequence-specific DNA analysis, Angew. Chem. Int. Ed. 48 (2009) 8670–8674.
[18] S.A. Yeung, R. Hobson, S. Biggs, F. Grieser, Formation of gold sols using ultrasound, J. Chem. Soc. Chem. Commun. (1993) 378–379.
[19] K. Okitsu, M. Ashokkumar, F. Grieser, Sonochemical synthesis of gold nanoparticles: effects of ultrasound frequency, J. Phys. Chem. B 109 (2005) 20673–20675.
[20] K. Okitsu, A. Yue, S. Tanabe, H. Matsumoto, Y. Yobiko, Formation of colloidal gold nanoparticles in an ultrasonic field: control of rate of gold(III) reduction and size of formed gold particles, Langmuir 17 (2001) 7717–7720.
[21] W. Haiss, N.T.K. Thanh, J. Aveyard, D.G. Fernig, Determination of size and concentration of gold nanoparticles from UV–vis spectra, Anal. Chem. 79 (2007) 4215–4221.
[22] P.B. Kandagal, S. Ashoka, J. Seetharamappa, S.M.T. Shaikh, Y. Jadegoud, O.B. Ijare, Study of the interaction of an anticancer drug with human and bovine serum albumin: spectroscopic approach, J. Pharm. Biomed. Anal. 41 (2006) 393–399.
[23] Y.Q. Wang, H.M. Zhang, G.C. Zhang, W.H. Tao, Z.H. Fei, Z.T. Liu, Spectroscopic studies on the interaction between silicotungstic acid and bovine serum albumin, J. Pharm. Biomed. Anal. 43 (2007) 1869–1875.
[24] H.A. Benesi, J.H. Hildebrand, A spectrophotometric investigation of the interaction of iodine with aromatic hydrocarbons, J. Am. Chem. Soc. 71 (1949) 2703–2707.
[25] D. Gao, Y. Tian, S. Bi, Y. Chen, A. Yu, H. Zhang, Studies on the interaction of colloidal gold and serum albumins by spectral methods, Spectrochim. Acta A: Mol. Biomol. Spectrosc. 62 (2005) 1203–1208.